LJNM ENVIROTECH SOLUTIONS

Strategy Development

Table of Contents

1. Introduction

Climate change is projected to impact drastically in southern African during the 21st century under low mitigation futures (Niang et al., 2014). African temperatures are projected to rise rapidly, in the subtropics at least at 1.5 times the global rate of temperature increase (James and Washington, 2013; Engelbrecht et al., 2015). Moreover, the southern African region is projected to become generally drier under enhanced anthropogenic forcing (Christensen et al., 2007; Engelbrecht et al., 2009; James and Washington, 2013; Niang et al., 2014). These changes in temperature and rainfall patterns will plausibly have a range of impacts in South Africa, including impacts on energy demand (in terms of achieving human comfort within buildings and factories), agriculture (e.g. reductions of yield in the maize crop under higher temperatures and reduced soil moisture), livestock production (e.g. higher cattle mortality as a result of oppressive temperatures) and water security (through reduced rainfall and enhanced evapotranspiration) (Engelbrecht et al., 2015).

It is important to realise that climate change is not to take place only through changes in average temperature and rainfall patterns, but also through changes in the attributes of extreme weather events. For the southern African region, generally drier conditions and the more frequent occurrence of dry spells are plausible (Christensen et al., 2007; Engelbrecht et al., 2009). Tropical cyclone tracks are projected to shift northward, bringing more flood events to northern Mozambique and fewer to the Limpopo province in South Africa (Malherbe et al., 2013). Cut-off low related flood events are also projected to occur less frequently over South Africa (e.g. Engelbrecht et al., 2013) in response to a poleward displacement of the westerly wind regime. Intense thunderstorms are plausible to occur more frequently over South Africa in a generally warmer climate (e.g. Engelbrecht et al., 2013).

The purpose of this report is to provide an update on the latest insights and evidence available regarding future changes in climatological averages and extreme events over South Africa, with a focus on changes that are to impact on the Free State province. Recent downscalings of global circulation model (GCM) projections of the Coupled Model Intercomparison Project Phase Five (CMIP5) and Assessment Report Five (AR5) of the Intergovernmental Panel on Climate Change (IPCC), obtained at the Council for Scientific and Industrial Research (CSIR) and the Commonwealth Scientific and Industrial Research Organisation (CSIRO), are used for this purpose. These downscalings are for the period 1971 to 2100, follow the experimental design recommended by the Coordinated Downscaling Experiment (CORDEX) and have been derived for both low and high mitigation scenarios. The regional climate model used to obtain the downscalings is the conformal-cubic atmospheric model (CCAM) of the CSIRO. In addition, the report also considers evidence on changes in extremes events over southern Africa as presented in Assessment Report Four (AR4) and AR5 of the IPCC (Christensen et al., 2007; Niang et al., 2014) and in the Long Term Adaptation Scenarios Report (LTAS, 2013) of the Department of Environmental Affairs (DEA).

2. Experimental design and model verification

Regional climate modelling is used to downscale the projections of CMIP5 GCMs to high resolution over southern Africa. The regional climate model used, CCAM, is a variable-resolution GCM developed by the CSIRO (McGregor 2005; McGregor and Dix 2001, 2008). The model solves the hydrostatic primitive equations using a semi-implicit semi-Lagrangian solution procedure, and includes a comprehensive set of physical parameterisations. The GFDL parameterisation for long-wave and shortwave radiation (Schwarzkopf and Fels 1991) is employed, with interactive cloud distributions determined by the liquid and ice-water scheme of Rotstayn (1997). The model employs a stability-dependent boundary layer scheme based on Monin-Obukhov similarity theory (McGregor et al. 1993). CCAM runs coupled to a dynamic land-surface model CABLE (CSIRO Atmosphere Biosphere Land Exchange model). The cumulus convection scheme uses mass-flux closure, as described by McGregor (2003), and includes both downdrafts and detrainment. CCAM may be employed in quasi-uniform mode or in stretched mode by utilising the Schmidt (1977) transformation.

Six GCM simulations of CMIP5 and AR5 of the IPCC, obtained for the emission scenarios described by Representative Concentration Pathways 4.5 and 8.5 (RCP4.5 – high mitigation and 8.5 – low mitigation) were downscaled to 50 km resolution globally. The simulations span the period 1971-2100. RCP4.5 is a high mitigation scenario, whilst RCP8.5 is a low mitigation scenario. The GCMs downscaled are the Australian Community Climate and Earth System Simulator (ACCESS1-0); the Geophysical Fluid Dynamics Laboratory Coupled Model (GFDL-CM3); the National Centre for Meteorological Research Coupled Global Climate Model, version 5 (CNRM-CM5); the Max Planck Institute Coupled Earth System Model (MPI-ESM-LR) and the Model for Interdisciplinary Research on Climate (MIROC4h). The simulations were performed on supercomputers of the CSIRO (Katzfey et al., 2012) and on the Centre for High Performance Computing (CHPC) of the Meraka Institute of the CSIR in South Africa.

In these simulations CCAM was forced with the bias-corrected daily sea-surface temperatures (SSTs) and sea-ice concentrations of each host model, and with CO_2, sulphate and ozone forcing consistent with the RCP4.5 and 8.5 scenarios. The model's ability to realistically simulate present-day southern African climate has been extensively demonstrated (e.g. Engelbrecht et al., 2009; Engelbrecht et al., 2011; Engelbrecht et al., 2013; Malherbe et al., 2013; Winsemius et al., 2014; Engelbrecht et al., 2015). Most current coupled GCMs do not employ flux corrections between atmosphere and ocean, which contributes to the existence of biases in their simulations of present-day SSTs – more than 2 ºC along the West African coast. The bias is computed by subtracting for each month the Reynolds (1988) SST climatology (for 1961-2000) from the corresponding GCM climatology. The bias-correction is applied consistently throughout the simulation. Through this procedure the climatology of the SSTs applied as lower boundary forcing is the same as that of the Reynolds SSTs. However, the intra-annual variability and climate-change signal of the GCM SSTs are preserved (Katzfey et al., 2009).

2.1.1. Model projections of the changing patterns of climate and extreme weather events over South Africa under enhanced anthropogenic forcing

In this section the projected changes in a number of climatological variables (Table 2.1), including extreme weather-events metrics, are presented. For each of the metrics under consideration, the simulated baseline (climatological) state over South Africa calculated for the period 1971-2000 is shown in a first figure (note that the median of the six downscalings is shown in this case). The projected changes in the metric are subsequently shown, for the time-slab 2020-2050 relative to the baseline period 1971-2000, first for RCP8.5 (low mitigation) and then for RCP4.5 (high mitigation). Three figures are presented for each metric for each RCP, namely the 10th, 50th (median) and 90th percentiles of the ensemble of projected changes under the RCP. In this way, it is possible to gain some understanding of the uncertainty range that is associated with the projections.

Table 2.1: Relevant climate variables

Variable	Description and/or units
Average temperature	°C
Very hot days	A day when the maximum temperature exceeds 35 °C. Units are number of events per grid point per year.
Heat-wave days	The maximum temperature exceeds the average temperature of the warmest month of the year by 5 °C for at least 3 days.
High fire-danger days	McArthur fire-danger index exceeds a value of 24. Units are number of events per grid point per year.
Rainfall	Mm
Extreme rainfall Type I event (also a proxy for lightning)	More than 20 mm of rain falling within 24 hrs over an area of 50 x 50 km^2. The occurrence of extreme convective rainfall is used as a proxy for the occurrence of storms that produce lightning. Units are number of events per grid point per year.
Dry-spell	Five or more consecutive days without rainfall (units are number of days per grid point per year)

3. Projected climate futures of the Free State

3.1. Average temperature

The model-simulated annual average temperatures (°C) are displayed in Figure 3.1 for the baseline period 1971-2000. The hottest regions are the western parts of the Free State.

- Rapid rises in the annual-average near-surface temperatures are projected to occur over southern Africa during the 21st century – temperatures over the South African interior are projected to rise at about 1.5 to 2 times the global rate of temperature increase (Engelbrecht et al., 2015).
- For the period 2020-2050 relative to the period 1971-2000, temperature increases of 1 to 2.5 °C are projected to occur over the Free State under low mitigation (Figure 3.2).
- Under high mitigation, temperature increases over the Free State province will be somewhat less, but may still reach 2.5 °Cover the western part of the province (Figure 3.2).
- Increasing temperatures over the Free State may plausibly increase the household demand for cooling over the coming decades.
- By the end of the century, temperature increases of 4 to 7 °C are projected to occur over the Free State under the RCP8.5 scenario (not shown). Such drastic temperature increases would have significant impacts on numerous sectors, including agriculture, water and energy.

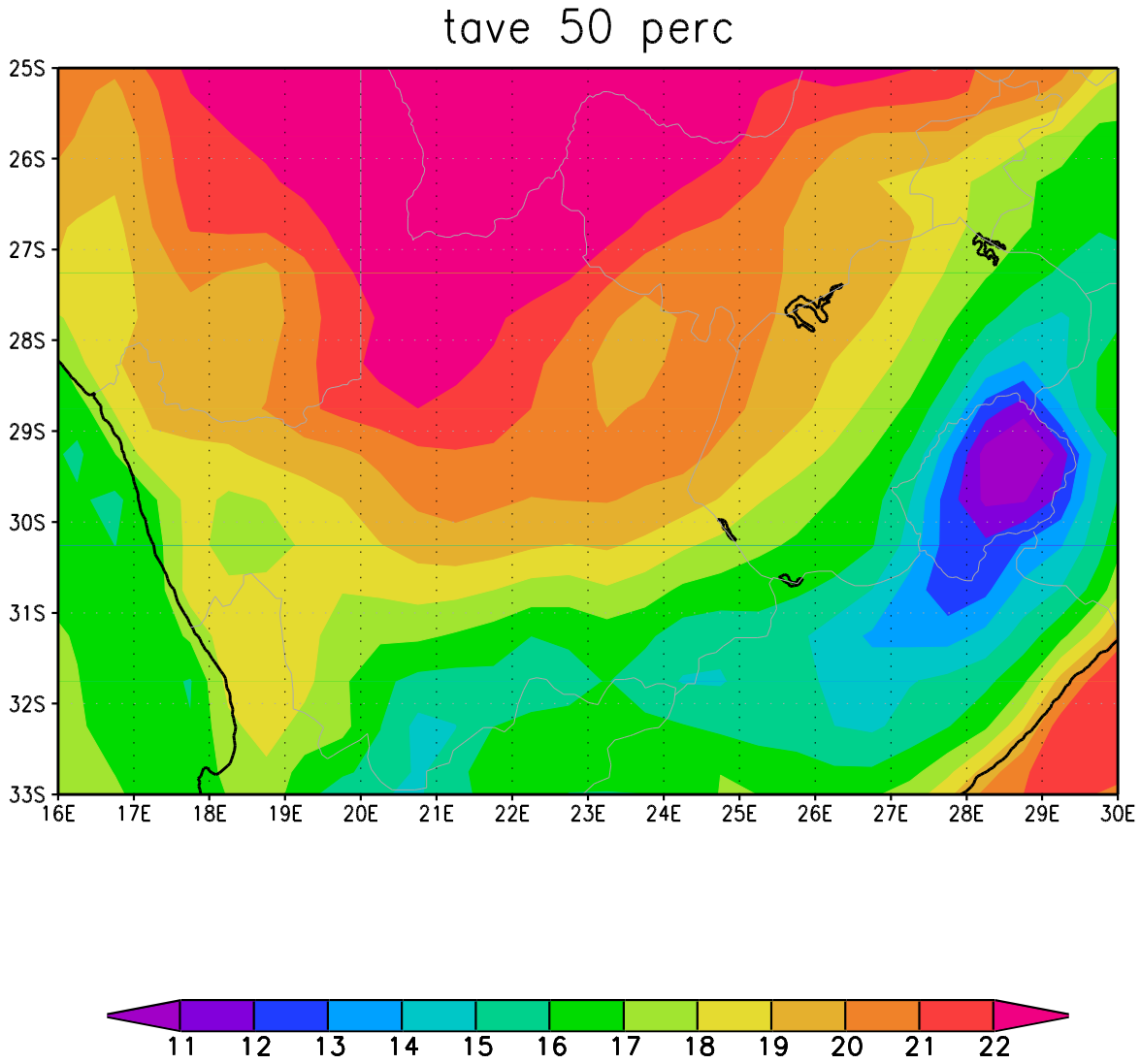

Figure 3.1: CCAM simulated annual average temperature (°C) over the Free State for the baseline period 1971-2000. The median of simulations is shown for the ensemble of downscalings of six GCM simulations.

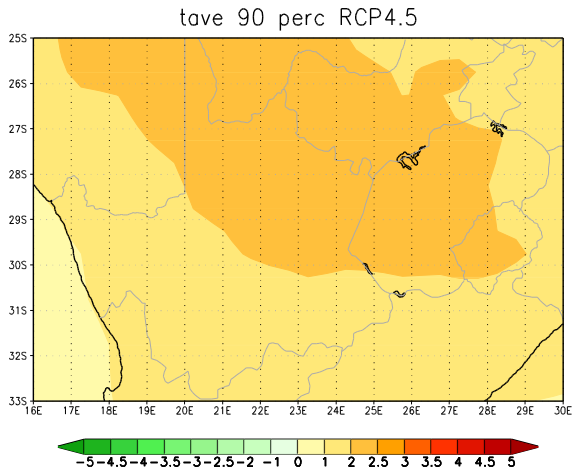
tave 90 perc RCP4.5
25S 26S 27S 28S 29S 30S 31S 32S 33S
16E 17E 18E 19E 20E 21E 22E 23E 24E 25E 26E 27E 28E 29E 30E
-5 -4.5 -4 -3.5 -3 -2.5 -2 -1 0 1 2 2.5 3 3.5 4 4.5 5

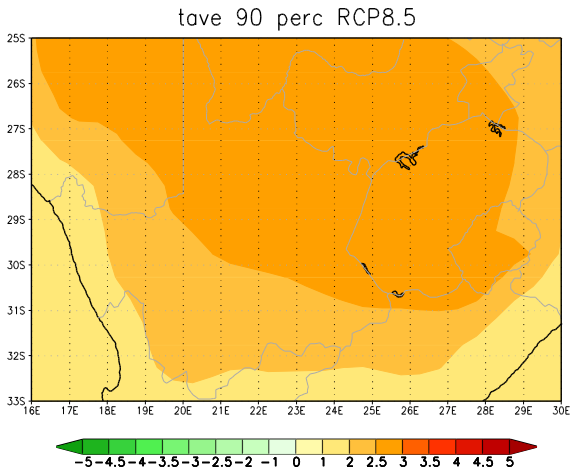
tave 90 perc RCP8.5
25S 26S 27S 28S 29S 30S 31S 32S 33S
16E 17E 18E 19E 20E 21E 22E 23E 24E 25E 26E 27E 28E 29E 30E
-5 -4.5 -4 -3.5 -3 -2.5 -2 -1 0 1 2 2.5 3 3.5 4 4.5 5

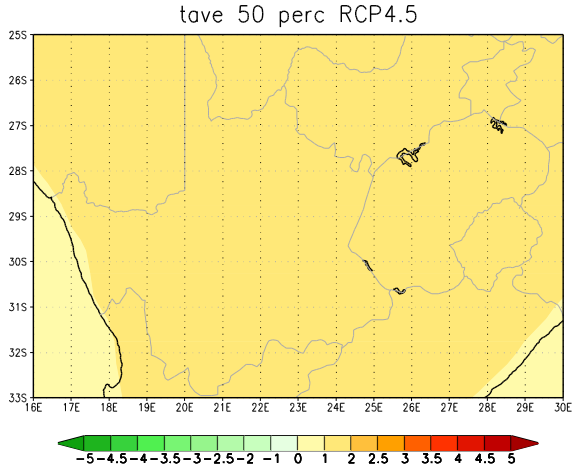
tave 50 perc RCP4.5
25S 26S 27S 28S 29S 30S 31S 32S 33S
16E 17E 18E 19E 20E 21E 22E 23E 24E 25E 26E 27E 28E 29E 30E
-5 -4.5 -4 -3.5 -3 -2.5 -2 -1 0 1 2 2.5 3 3.5 4 4.5 5

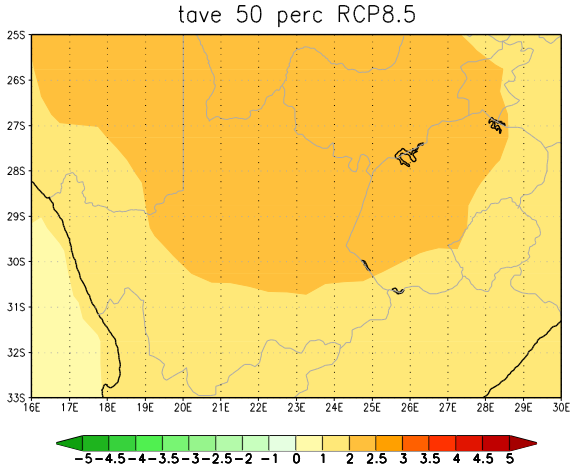
tave 50 perc RCP8.5
25S 26S 27S 28S 29S 30S 31S 32S 33S
16E 17E 18E 19E 20E 21E 22E 23E 24E 25E 26E 27E 28E 29E 30E
-5 -4.5 -4 -3.5 -3 -2.5 -2 -1 0 1 2 2.5 3 3.5 4 4.5 5

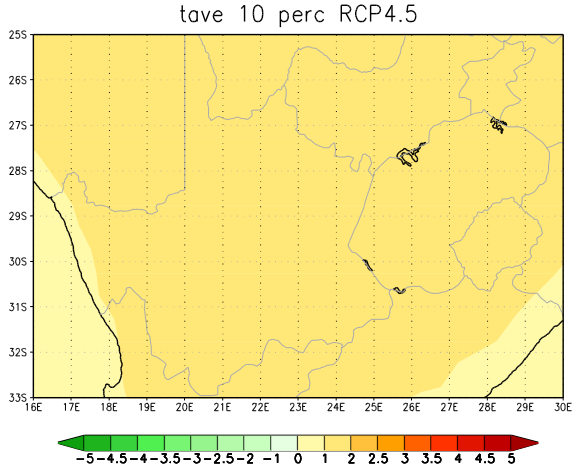
tave 10 perc RCP4.5
25S 26S 27S 28S 29S 30S 31S 32S 33S
16E 17E 18E 19E 20E 21E 22E 23E 24E 25E 26E 27E 28E 29E 30E
-5 -4.5 -4 -3.5 -3 -2.5 -2 -1 0 1 2 2.5 3 3.5 4 4.5 5

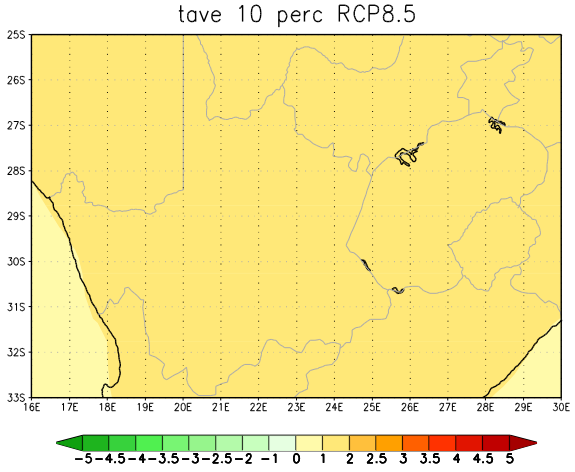
tave 10 perc RCP8.5
25S 26S 27S 28S 29S 30S 31S 32S 33S
16E 17E 18E 19E 20E 21E 22E 23E 24E 25E 26E 27E 28E 29E 30E
-5 -4.5 -4 -3.5 -3 -2.5 -2 -1 0 1 2 2.5 3 3.5 4 4.5 5

Figure 3.2: CCAM projected change in the annual average temperature (°C) over the Free State for the time-slab 2020-2050 relative to 1971-2000. The 10th, 50th and 90th percentiles are shown for the ensemble of downscalings of six GCM projections under RCP4.5 (left) and RCP8.5 (right).

3.2. Very hot days

The model-simulated and bias-corrected annual average number of very hot days (days when the maximum temperature exceeds 35 °C, units are number of days per model grid point) are displayed in Figure 3.3, for the baseline period 1971-2000. Over the western Free State, more than 70 very hot days occur on the average annually.

- In association with drastically rising maximum temperatures (Figure 3.4.), the frequency of occurrence of very hot days is also projected to increase drastically under climate change.
- For the period 2020-2050 relative to 1971-1990, under low mitigation, very hot days are projected to increase with as many as 70 days per year in the western part of the Free State (Figure 3.4). More modest increases are projected for the eastern parts.
- Even under high mitigation, the increase in the number of very hot days may be as high as 40 days over the western Free State (Figure 3.4).
- Increases in the occurrence of very hot days occur in association with projected changes in the frequency of occurrence of heat-wave days and high fire-danger days (see sections 3.3 and 3.4). These changes may impact on human and animal health through increased heat stress, are likely to impact negatively on crop yield and are conducive to the occurrence of veld and forest fires.

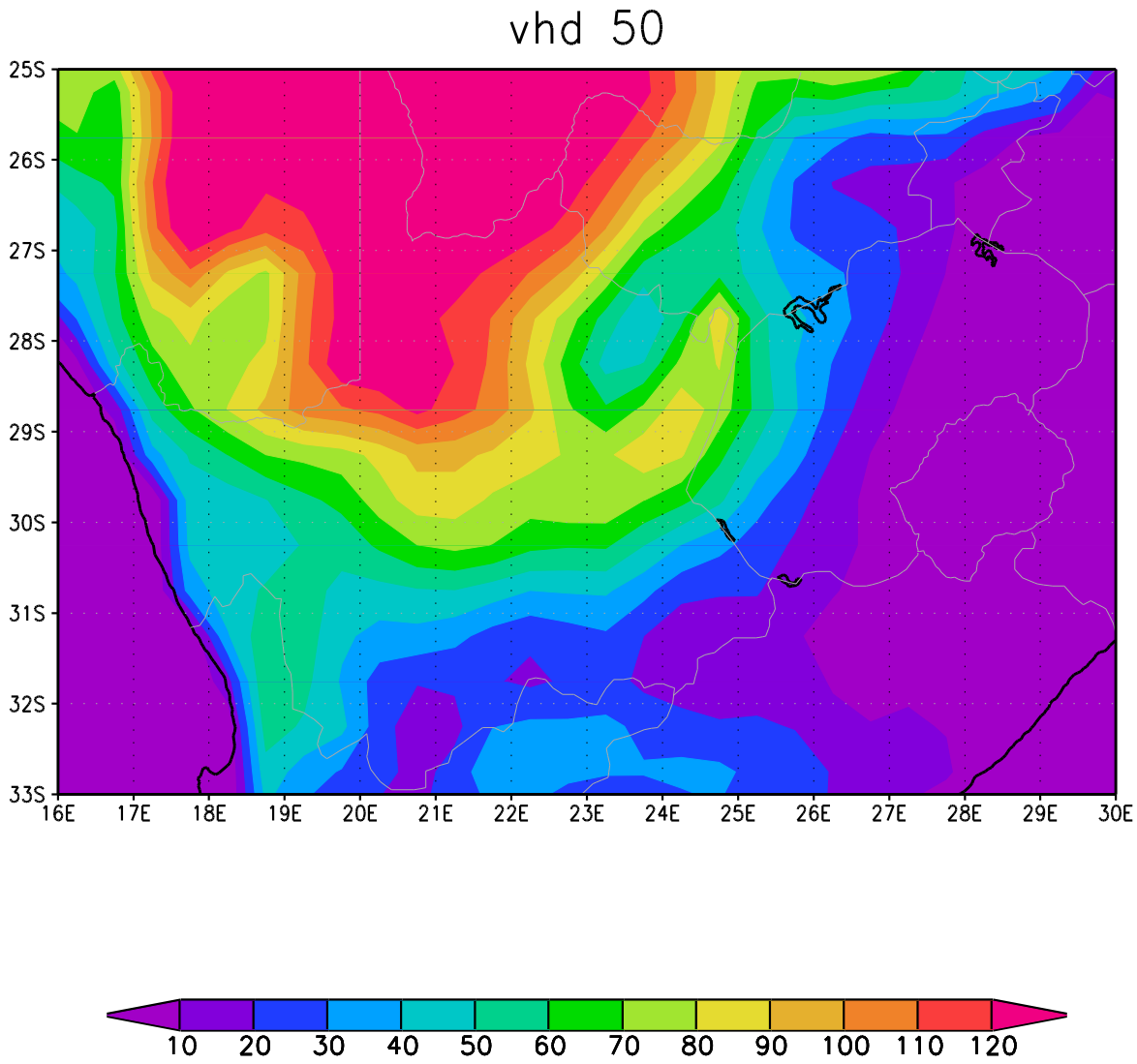

Figure 3.3: CCAM simulated annual average number of very hot days (units are number of days per grid point per year) over the Free State for the baseline period 1971-2000. The median of simulations is shown for the ensemble of downscalings of six GCM simulations.

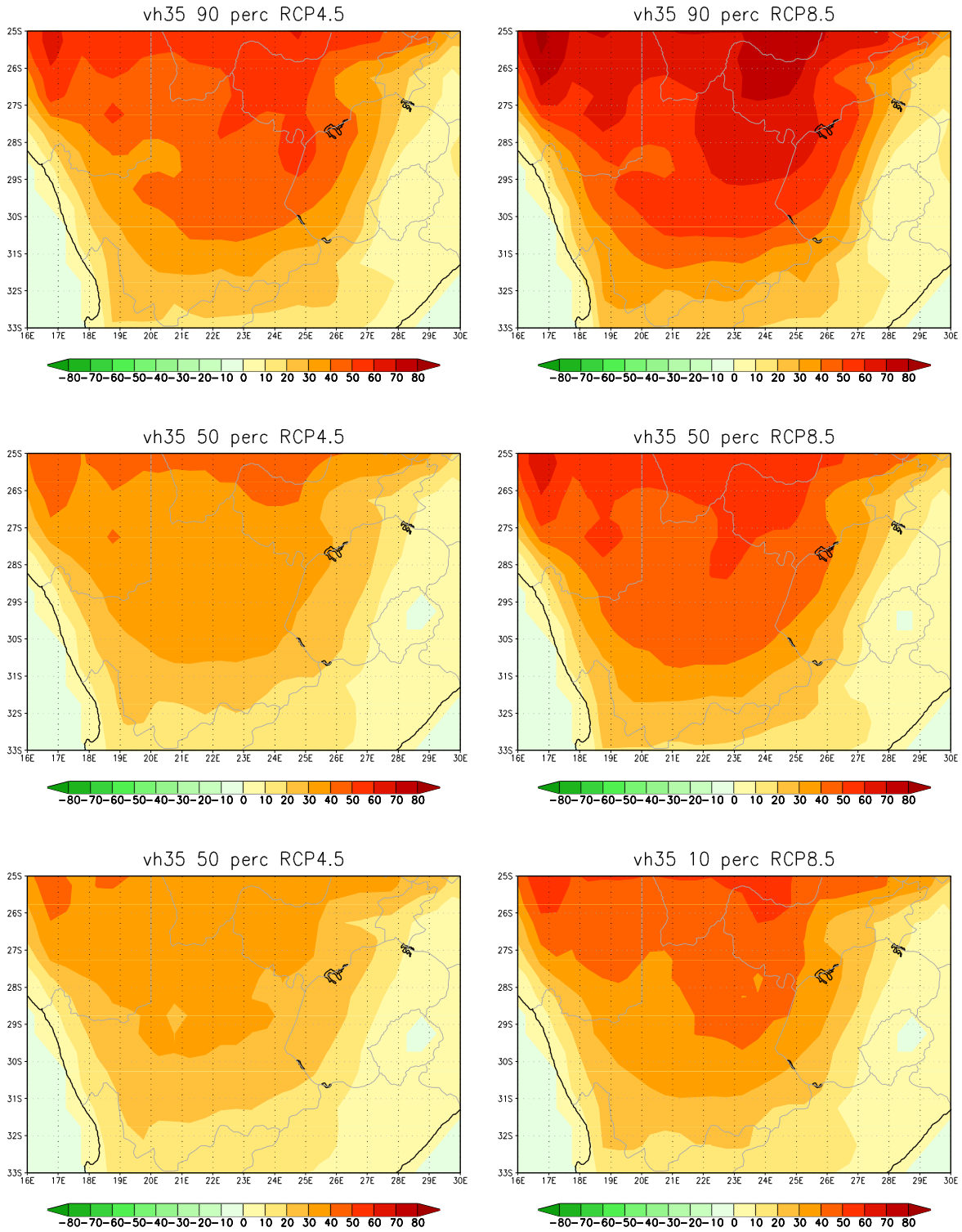

Figure 3.4: CCAM projected change in the annual average number of very hot days (units are days per grid point per year) over the Free State for the time-slab 2021-2050 relative to 1971-

2000. The 10th, 50th and 90th percentiles are shown for the ensemble of downscalings of six GCM projections under RCP4.5 (left) and RCP8.5 (right).

3.3. Heat-wave days

The model-simulated annual-average numbers of heat-wave days (units are number of days per model grid point) are displayed in Figure 3.5, for the baseline period 1971-2000. A heat-wave is defined as an event when the maximum temperature at a specific location exceeds the average maximum temperature of the warmest month of the year at that location by 5 °C, for a period of at least three days. To the total number of days occurring within a heat-wave is referred to as "heat-wave days". Heat-waves are rare events in terms of southern Africa's present-day climate, with most of the Free State experiencing less than ten of these days per annum. The highest heat-wave day frequencies occur over the eastern parts of the province.

- In association with drastically rising maximum temperatures (Figure 3.6), the frequency of occurrence of heat-wave days are also projected to increase drastically under climate change.
- For the period 2020-2050 relative to 1971-2000, under low mitigation, heat-wave days may increase by as many as 20-30 days per year over large parts of the Free State (Figure 3.6).
- Even under high mitigation, the increase in the number of heat-wave days may be 20 or more over the eastern parts of the province (Figure 3.6).
- Increases in the occurrence of heat-wave days occur in association with projected changes in the frequency of very hot days and high fire-danger days (see section 3.2 and 3.4). Since heat-wave days are associated with prolonged periods of oppressive temperatures, these changes may impact on human and animal health through increased heat stress, are likely to impact negatively on crop yield and are plausible to be conducive to the occurrence of veld and forest fires.

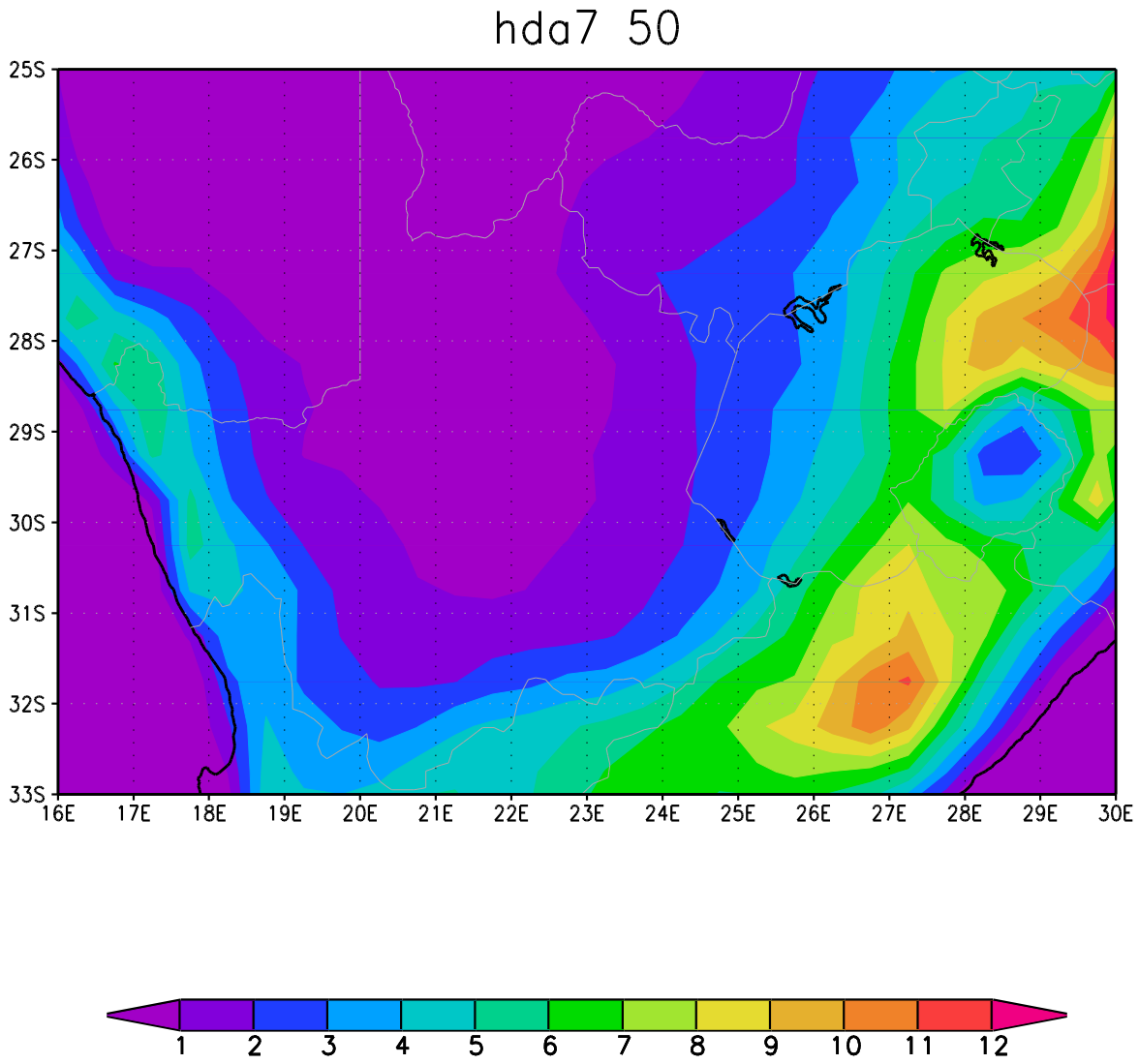

Figure 3.5: CCAM simulated annual average number of heat-wave days (units are number of days per grid point per year) over the Free State and Nothwest, for the baseline period 1971-2000. The median of simulations is shown for the ensemble of downscalings of six GCM simulations.

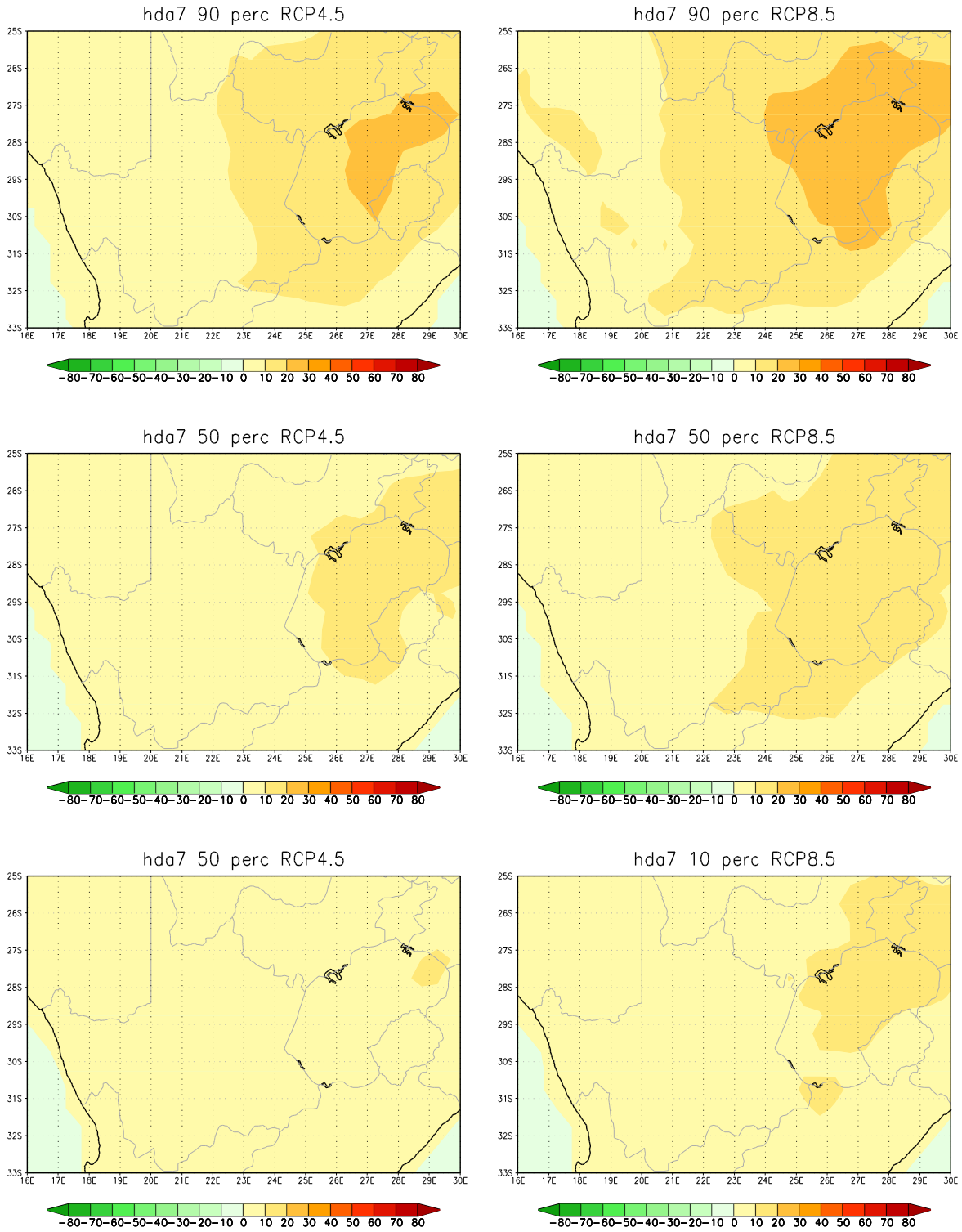

Figure 3.6: CCAM projected change in the annual average number of heat-wave days (units are number of days per grid point per year) over the Free State for the time-slab 2020-2050

relative to 1971-2000. The 10th, 50th and 90th percentiles are shown for the ensemble of downscalings of six GCM projections under RCP4.5 (let) and RCP8.5 (right).

3.4. High fire-danger days

The model-simulated annual average number of high fire-danger days (days when the McArthur Fire Danger Index exceeds a value of 24, units are number of days per model grid point) are displayed in Figure 3.7, for the baseline period 1971-2000. Over the western grasslands of the Free State 20-80 high fire-danger days occur on the average per year.

- In association with drastically rising temperatures (Figure 3.2), the frequency of occurrence of high fire-danger days are also projected to increase drastically under climate change (Figure 3.8).
- For the period 2020-2050 relative to 1971-2000, under low mitigation, it is plausible that high fire-danger will increase with 80 days per year (or more) over the western Free State grasslands (Figure 3.8).
- Even under high mitigation, the increase in the number of high fire-danger days may approach 80 days over the western parts of the province (Figure 3.8).
- Increases in the occurrence of high fire-danger days occur in association with projected changes in the frequency of occurrence of heat-wave days (section 3.3)and high fire danger days.

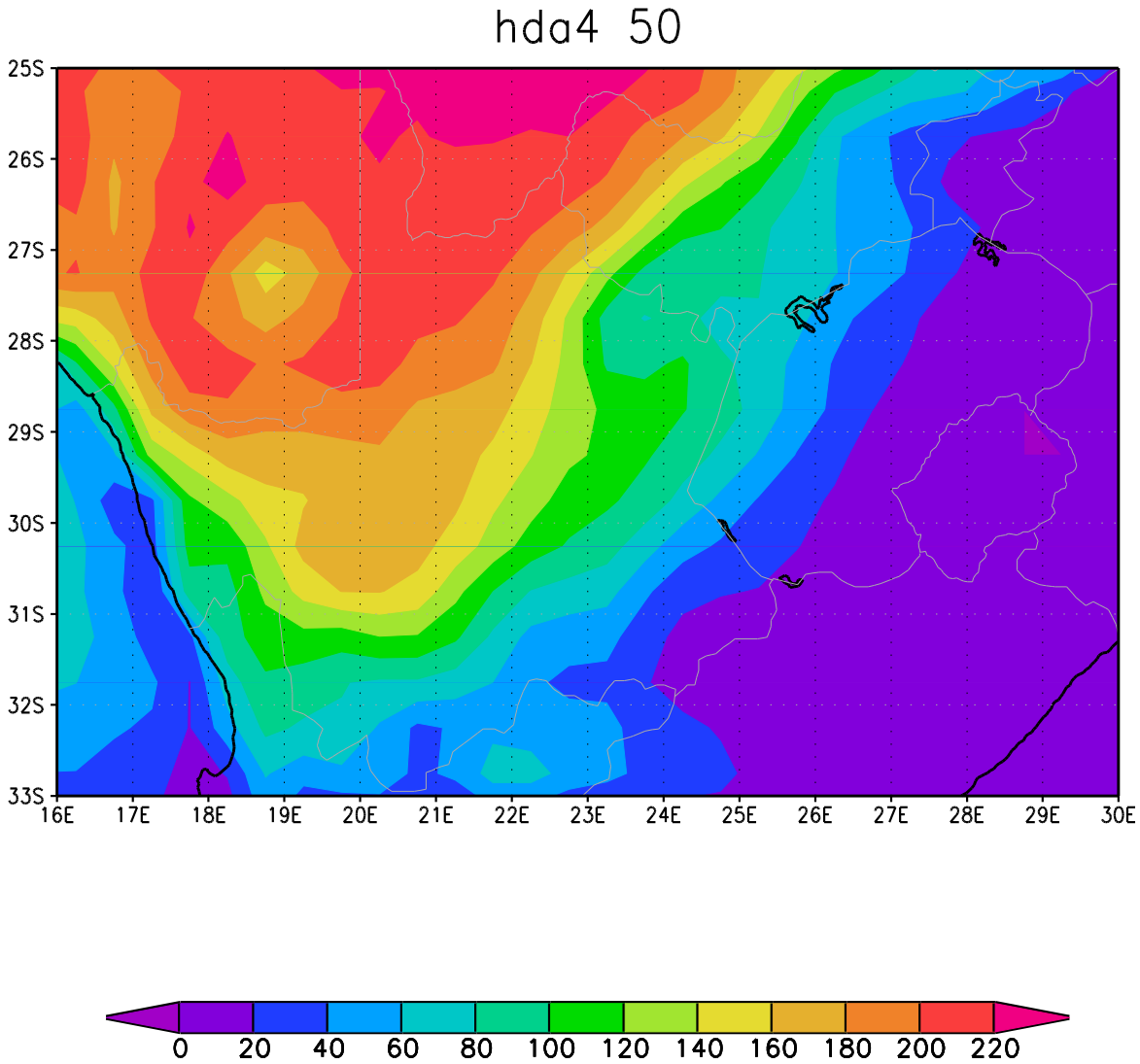

Figure 3.7: CCAM simulated annual average number of high fire-danger days (units are number of days per grid point per year) over the Free State for the baseline period 1971-2000. The median of simulations is shown for the ensemble of downscalings of six GCM simulations.

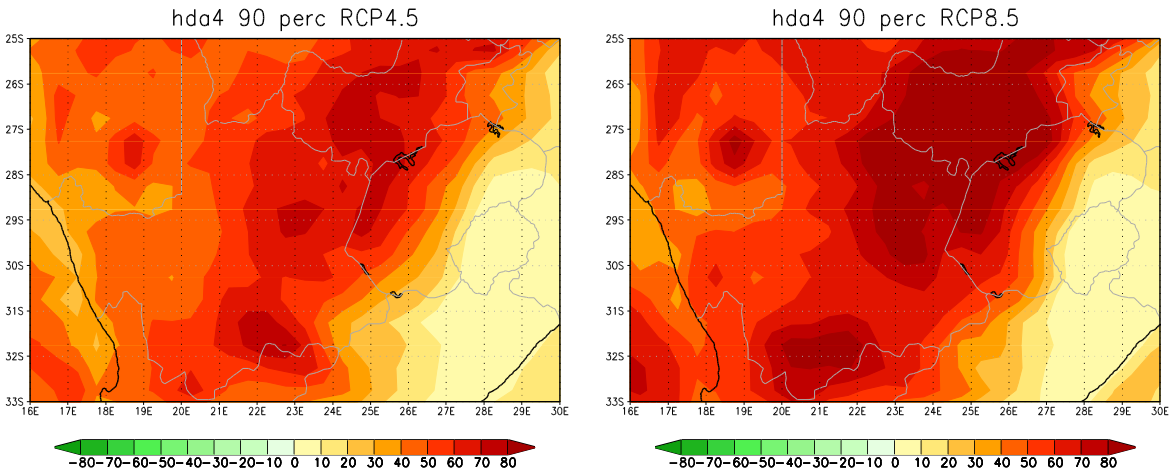
hda4 90 perc RCP4.5
hda4 90 perc RCP8.5
25S 26S 27S 28S 29S 30S 31S 32S 33S
16E 17E 18E 19E 20E 21E 22E 23E 24E 25E 26E 27E 28E 29E 30E
−80 −70 −60 −50 −40 −30 −20 −10 0 10 20 30 40 50 60 70 80

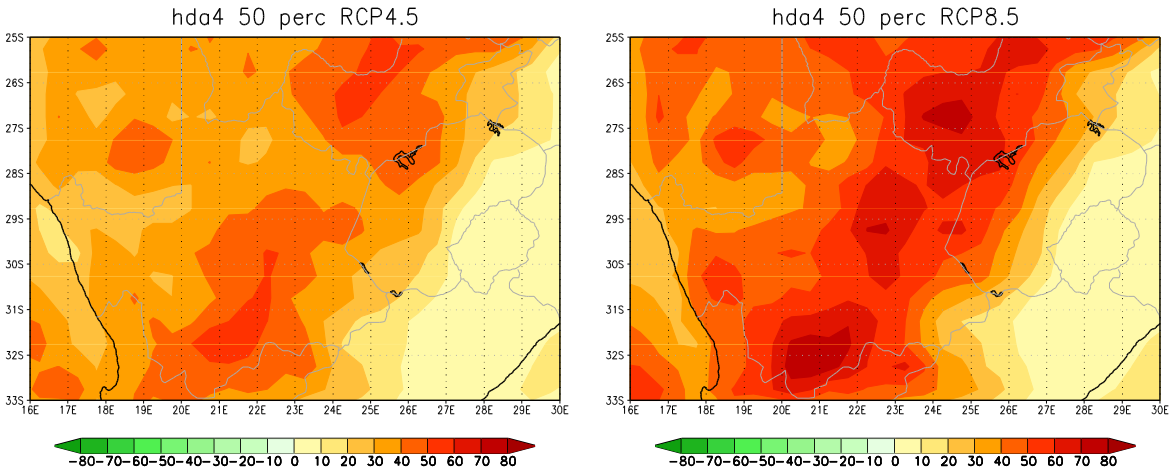
hda4 50 perc RCP4.5
hda4 50 perc RCP8.5
25S 26S 27S 28S 29S 30S 31S 32S 33S
16E 17E 18E 19E 20E 21E 22E 23E 24E 25E 26E 27E 28E 29E 30E
−80 −70 −60 −50 −40 −30 −20 −10 0 10 20 30 40 50 60 70 80

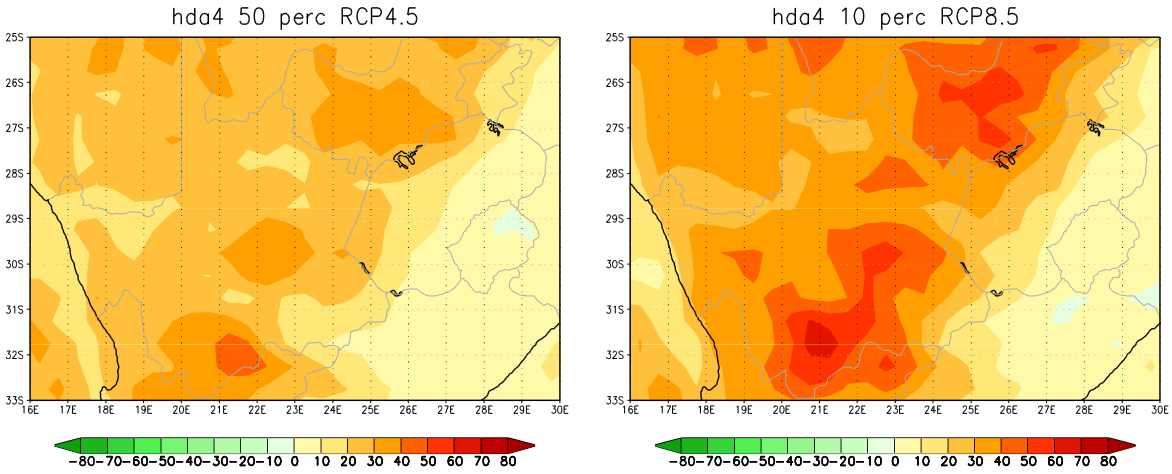
hda4 50 perc RCP4.5
hda4 10 perc RCP8.5
25S 26S 27S 28S 29S 30S 31S 32S 33S
16E 17E 18E 19E 20E 21E 22E 23E 24E 25E 26E 27E 28E 29E 30E
−80 −70 −60 −50 −40 −30 −20 −10 0 10 20 30 40 50 60 70 80

Figure 3.8: CCAM projected change in the annual average number of high fire-danger days (units are number of days per grid point per year) over the Free State for the time-slab 2021-2050 relative to 1971-2000. The 10th, 50th and 90th percentile are shown for the ensemble of downscalings of six GCM projections under RCP4.5 (left) and RCP8.5 (right).

3.5. Rainfall

The model-simulated annual average rainfall totals (mm) are displayed in Figure 3.9, for the baseline period 1971-2000. There is a pronounced west-east rainfall gradient over the country, which also extends over the Free State.

- A general decrease in rainfall is plausible over southern Africa under enhanced anthropogenic forcing (e.g. Christensen et al., 2007; Engelbrecht et al., 2009).
- Uncertainty surrounds the projected rainfall futures of the Free State. For the period 2020-2050 relative to the period 1971-2000, under low mitigation, rainfall is projected to decrease significantly (more than 40 mm per year) by some ensemble members, whilst other ensemble members are projecting rainfall increases of more than 40 mm per year (Figure 3.10).
- The projected changes in rainfall patterns under high mitigation are very similar to the patterns projected under low mitigation (Figure 3.10).
- The projected changes in rainfall patterns over South Africa in the ensemble of downscalings described here, and more generally in AR4 and AR5 projections, display more uncertainty than in the case of projected changes in temperature. This implies that adaptation policy makers need to take into account a range of different rainfall futures, often of different signal (i.e. drier and wetter) during the decision making process.

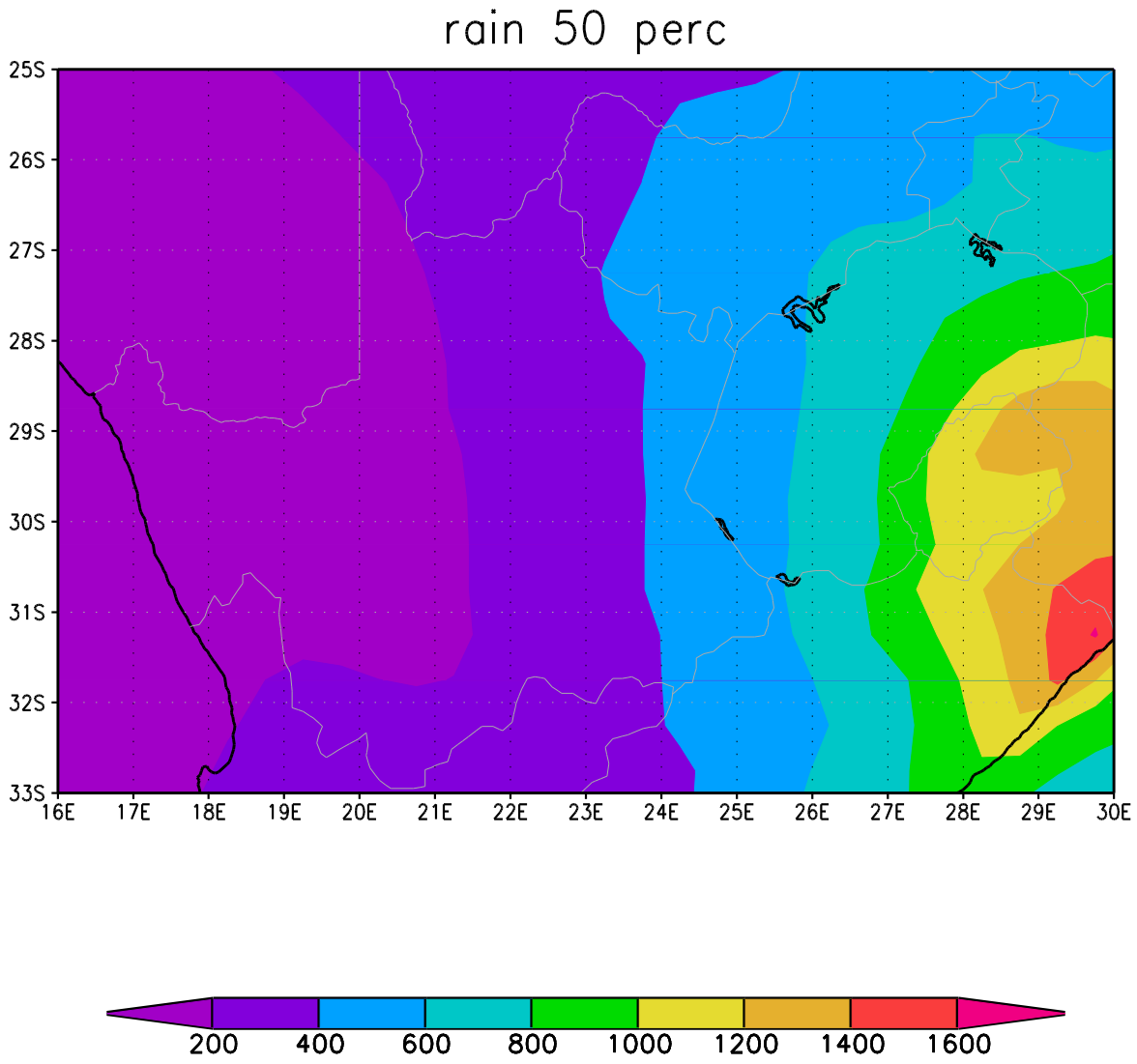

Figure 3.9: CCAM simulated annual average rainfall totals (mm) over the Free State for the baseline period 1971-2000. The median of simulations is shown for the ensemble of downscalings of six GCM simulations.

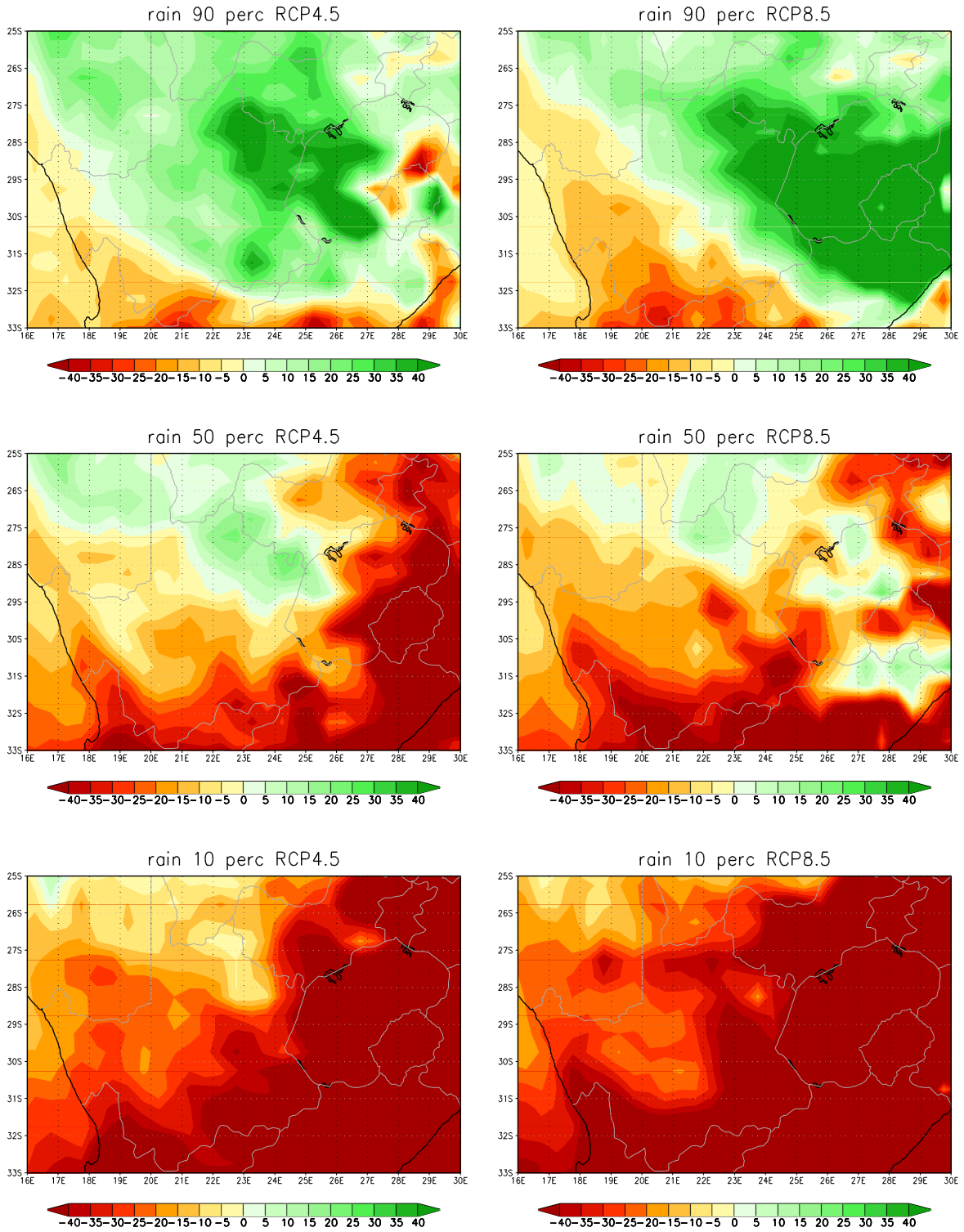

Figure 3.10: CCAM projected change in the annual average rainfall totals (mm) over central South Africa, for the time-slab 2020-2050 relative to 1971-2000. The 10th, 50th and 90th

percentiles are shown for the ensemble of downscalings of six GCM projections under RCP4.5 (left) and RCP8.5 (right).

3.6. Extreme rainfall events (including severe thunderstorms and lightning)

The model-simulated annual average extreme rainfall event frequencies (units are number of events per model grid box per year) are displayed in Figure 3.11, for the baseline period 1971-2000. Here an extreme rainfall event is defined as 20 mm of rain occurring within 24 hours over an area of 50 x 50 km^2). Over the eastern parts of the province up to 16 extreme rainfall events occur annually, on the average.

- Extreme rainfall events are projected to decrease in frequency over the Free State under low mitigation, for the period 2020-2050 relative to 1971-2000, by most ensemble members (Figure 3.12). A minority of ensemble members project increases in extreme rainfall events over the Free State (Figure 3.12).
- The projected changes in extreme rainfall events under high mitigation are very similar to the patterns projected under low mitigation (Figure 3.12).
- Extreme rainfall events are mostly caused by intense thunderstorms, which are often also the cause of lightning, hail, damaging winds and flash floods. That is, the climate change projections analysed here are indicative that decreases in these hazardous storms are plausible over most of the Free State, however, a minority of ensemble members are indicative of increases in such events. That is, adaptation policies need to take into account the possibility that extreme rainfall events over the Free State may increase in their frequency of occurrence.

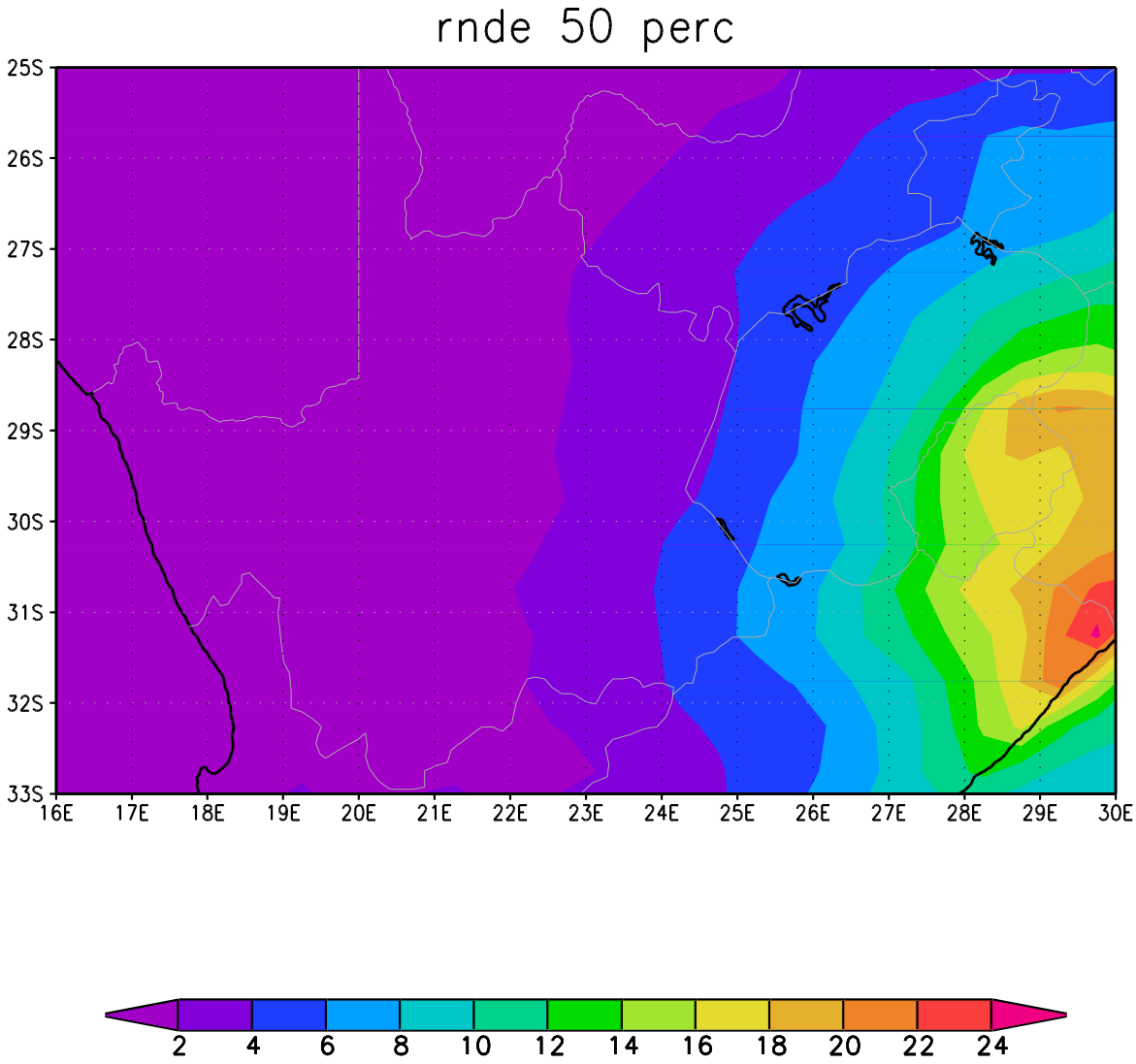

Figure 3.11: CCAM simulated annual average number of extreme rainfall days (units are number of days per grid point per year) over the Free State for the baseline period 1971-2000. The median of simulations is shown for the ensemble of downscalings of six GCM simulations.

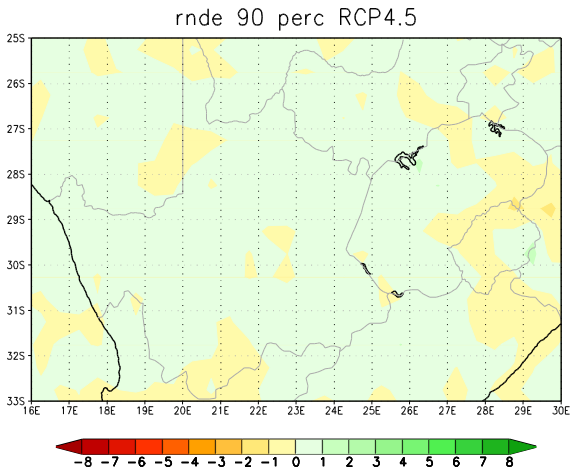
rnde 90 perc RCP4.5
25S 26S 27S 28S 29S 30S 31S 32S 33S
16E 17E 18E 19E 20E 21E 22E 23E 24E 25E 26E 27E 28E 29E 30E
-8 -7 -6 -5 -4 -3 -2 -1 0 1 2 3 4 5 6 7 8

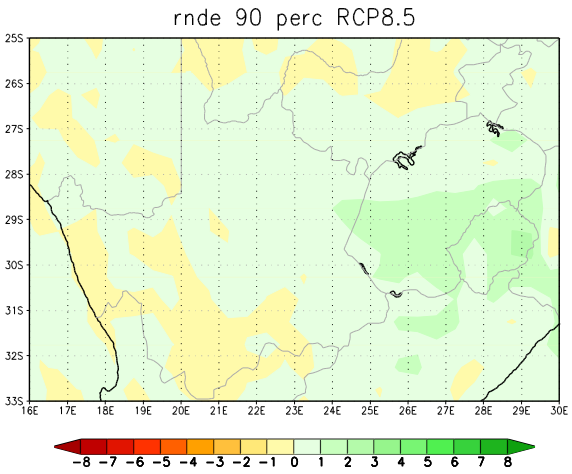
rnde 90 perc RCP8.5
25S 26S 27S 28S 29S 30S 31S 32S 33S
16E 17E 18E 19E 20E 21E 22E 23E 24E 25E 26E 27E 28E 29E 30E
-8 -7 -6 -5 -4 -3 -2 -1 0 1 2 3 4 5 6 7 8

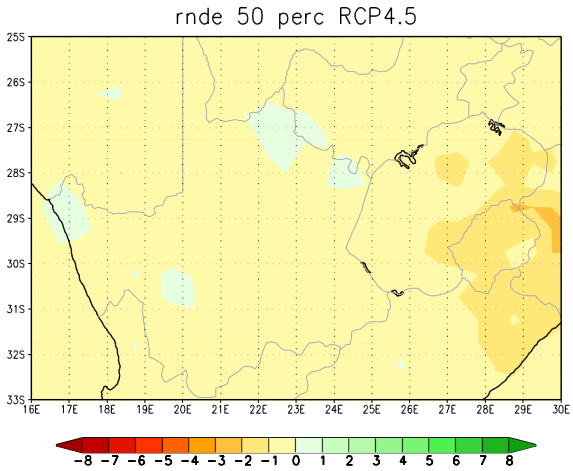
rnde 50 perc RCP4.5
25S 26S 27S 28S 29S 30S 31S 32S 33S
16E 17E 18E 19E 20E 21E 22E 23E 24E 25E 26E 27E 28E 29E 30E
-8 -7 -6 -5 -4 -3 -2 -1 0 1 2 3 4 5 6 7 8

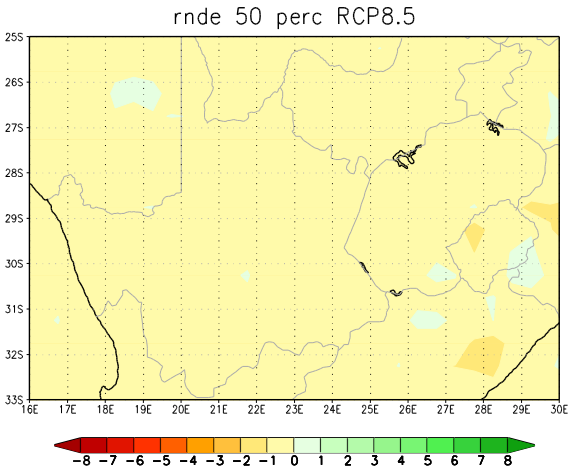
rnde 50 perc RCP8.5
25S 26S 27S 28S 29S 30S 31S 32S 33S
16E 17E 18E 19E 20E 21E 22E 23E 24E 25E 26E 27E 28E 29E 30E
-8 -7 -6 -5 -4 -3 -2 -1 0 1 2 3 4 5 6 7 8

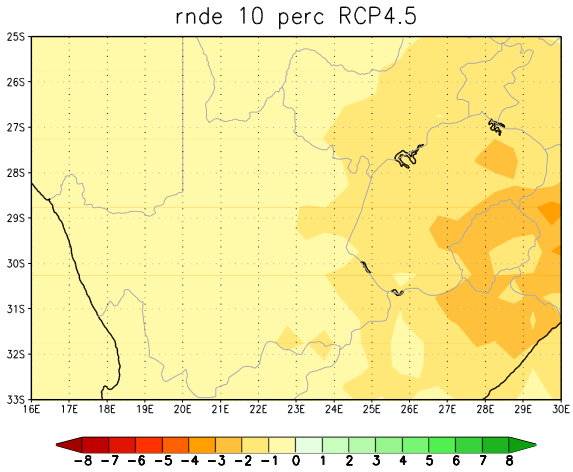
rnde 10 perc RCP4.5
25S 26S 27S 28S 29S 30S 31S 32S 33S
16E 17E 18E 19E 20E 21E 22E 23E 24E 25E 26E 27E 28E 29E 30E
-8 -7 -6 -5 -4 -3 -2 -1 0 1 2 3 4 5 6 7 8

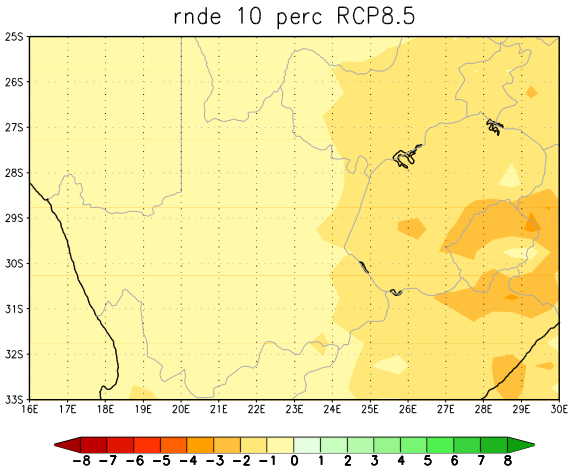
rnde 10 perc RCP8.5
25S 26S 27S 28S 29S 30S 31S 32S 33S
16E 17E 18E 19E 20E 21E 22E 23E 24E 25E 26E 27E 28E 29E 30E
-8 -7 -6 -5 -4 -3 -2 -1 0 1 2 3 4 5 6 7 8

Figure 3.12: CCAM projected change in the annual average number of extreme rainfall days (units are numbers of grid points per year) over central South Africa, for the time-slab 2020-2050 relative to 1971-2000. The 10th, 50th and 90th percentiles are shown for the ensemble of downscalings of six GCM projections under RCP8.5.

3.7. Dry spell days

The model-simulated annual average dry-spell day frequencies (units are number of days per model grid box per year) are displayed in Figure 3.13, for the baseline period 1971-2000. Here a dry spell is defined as a period of five consecutive days without rainfall (or a longer dry period) occurring over an area of 50 x 50 km^2. The days that constitute a dry spell event are termed “dry spell days”. South Africa receives seasonal rainfall over most of the country, implying that most locations experience a dry season exhibiting many dry spell days. The dry spell day gradient over South Africa resembles the rainfall gradient.

- The ensemble of downscalings is robust in projecting an increase in dry spell days over the Free State for the period 2020-2050 relative to 1971-2000, under low mitigation (Figure 3.14).
- The projected changes in dry spell day frequencies under high mitigation are very similar to the patterns projected under low mitigation (Figure 3.14).

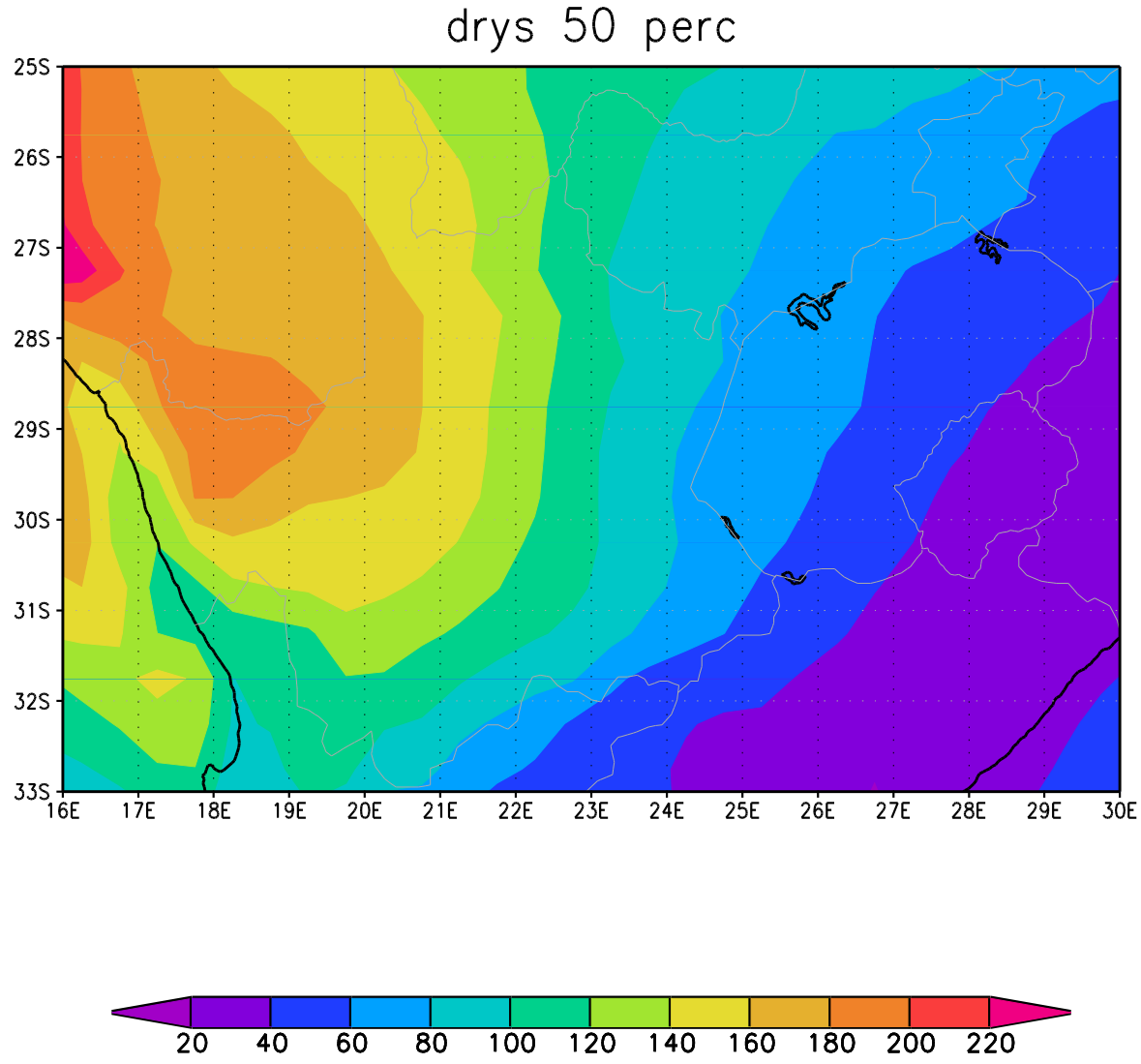

Figure 3.13: CCAM simulated annual average number of dry-spell days (units are number of days per grid point per year) over central South Africa, for the baseline period 1971-2000. The median of simulations is shown for the ensemble of downscalings of six GCM simulations.

drys 90 perc RCP4.5

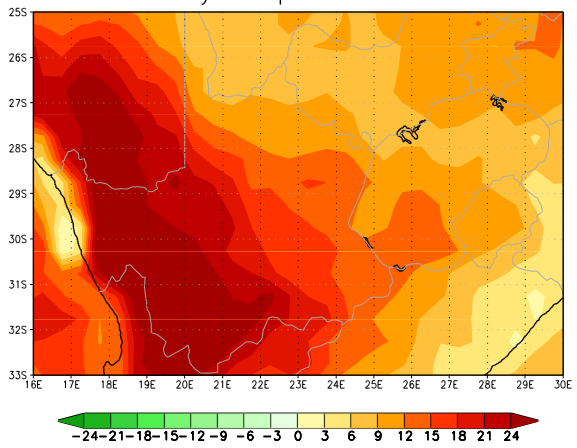

drys 90 perc RCP8.5

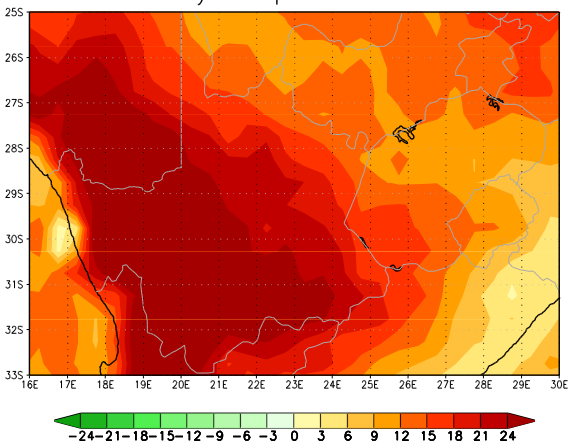

drys 50 perc RCP4.5

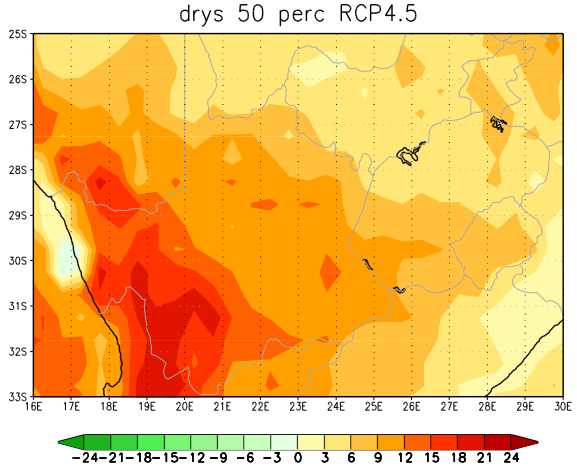

drys 50 perc RCP8.5

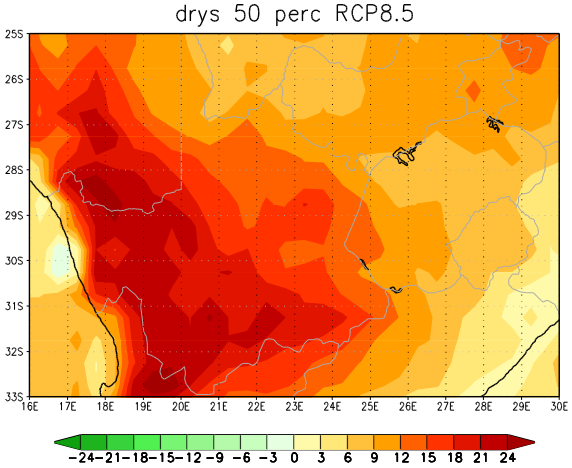

drys 10 perc RCP4.5

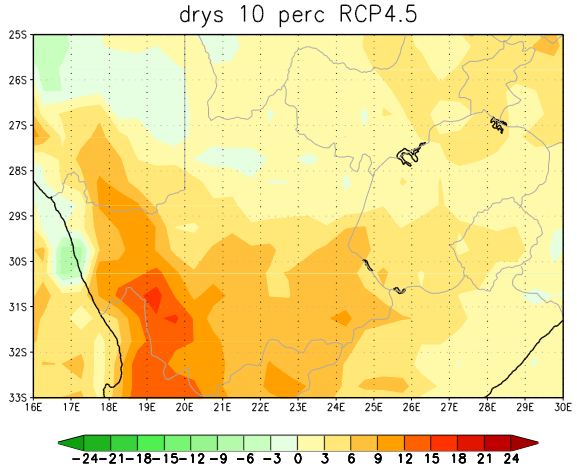

drys 10 perc RCP8.5

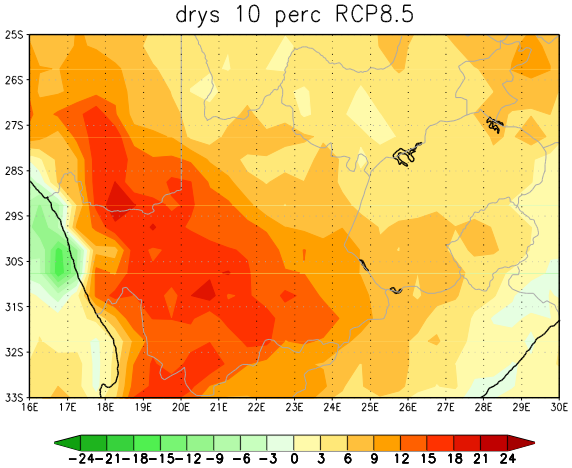

Figure 3.14: CCAM projected change in the annual average number of dry-spell days (units are numbers of grid points per year) over South Africa, for the time-slab 2021-2050 relative to 1971-2000. The 10th, 50th and 90th percentiles are shown for the ensemble of downscalings of six GCM projections under RCP4.5 (left) and RCP8.5 (right).

4. Conclusion

This report is based on an ensemble of high-resolution projections of future climate change over Africa, obtained by using the regional climate model CCAM to downscale the output of a number of CMIP5 (AR5) GCMs over Africa. The projections downscaled represent both high (RCP4.5) and low (RCP8.5) mitigation scenarios. CCAM was applied at 50 km resolution globally, and the experimental design of the simulations is consistent with that of CORDEX. The projections obtained are interpreted within the context of the GCM projections described in AR4 and AR5 of the IPCC and the regional projections of LTAS of DEA. The projected changes are presented for the period 2021-2050 relative to the 1971-2000 baseline period.

Under low mitigation, temperatures are projected to rise drastically, by 1-3 °C over the central South African interior for the period 2020-2050 relative to the baseline period. These increases are to be associated with increases in the number of very hot days, heat-wave days and high fire-danger days over South Africa. Key implications of these changes for Free State may include an increased risk for veld fires to occur in the grasslands areas. The household demand for energy in summer is also plausible to increase, to satisfy an increased cooling need towards achieving human comfort within buildings. Under high mitigation, the amplitudes of the projected changes in temperature and extreme temperature events are somewhat less, but still significant. The projected changes in rainfall and related extreme events exhibit more uncertainty than the projected temperature changes. A robust signal of increases in dry-spell-day frequencies is evident from the projections.